

# Effects of prestressing force on natural frequency of prestressed concrete beams considering self-weight

Soobong Shin<sup>1a</sup>, Hokyoung Lee<sup>2b</sup> and Jong-Han Lee<sup>\*1</sup>

<sup>1</sup>Department of Civil Engineering, Inha University, 100 Inha-ro, Michuhol-gu, Incheon 22212, Korea

<sup>2</sup>Korea Bridge Institute Co., 252 Gilju-ro, Wonmi-gu, Bucheon, Gyeonggido 14548, Korea

(Received July 27, 2019, Revised December 9, 2019, Accepted December 20, 2019)

**Abstract.** This study investigated the effects of prestressing force on the natural frequency of concrete beams considering changes in the self-weight of the beam. For this, a finite element formulation was derived to account for the increase in the stiffness of a beam-tendon system due to the axial force and deformation induced by prestressing of the tendon. The developed finite element formulation was validated with the data obtained in laboratory experiments. The experimental natural frequencies of the small prestressed concrete (PSC) beam specimens were consistent with those obtained using the proposed method. The first natural frequency increased almost linearly as the prestressing force increased. The proposed method was then applied to four actual PSC bridges typically employed in the field. Different from the laboratory specimens, the first natural frequencies of the actual PSC bridges barely changed or increased with increasing prestressing force. The results of an analytical parametric study showed that the increase in the natural frequency strongly depended on the magnitude of the prestressing force relative to the total weight of the structure. Thus, the variation in the natural frequencies of the actual PSC bridges with high total weight relative to the prestressing force was negligible due to the application of the prestressing force.

**Keywords:** prestressed concrete bridge; prestressing force; self-weight; natural frequency; geometric stiffness

## 1. Introduction

The dynamic response of a structure depends mainly on its mass and stiffness properties. Seo and Linzell (2011, 2012) investigated the dynamic characteristics of prestressed and curved bridges using computation models. In addition, Rogers and Seo (2016) assessed vulnerable sensitivity with various configurations subjected to multiple ground motions, and Lee *et al.* (2017) proposed experimental and measurement methods for the lateral and torsional stability of a precast girder. Variations in the material and sectional properties of a structure can induce considerable changes in the response of the structure (Gao *et al.* 2017, Turkeli *et al.* 2017). Theoretically, changes in the dynamic response of a structure are associated with changes in modal information. Thus, modal data of the natural frequencies and mode shapes of a structure are typically used to evaluate the dynamic characteristics of the structure (Abbasnia 2015, Goremikins *et al.* 2013, Noble 2015, Noh *et al.* 2015). In particular, the natural frequencies are widely used as an index to evaluate any changes in a structure (Shin 2010).

When a prestressed concrete (PSC) beam is subjected to an additional force due to prestressing of the beam, the

modal information of the beam is generally considered to change with changes in the stiffness of the beam rather than the mass. Several theoretical and experimental studies (Falati and Williams 1998, Hop 1991, James *et al.* 1964, Nabil and Ross 1996) additionally demonstrated that the natural frequency of a structure changes owing to the prestressing force. All of the experiments were conducted on PSC beam specimens to examine the influence of prestressing force on the natural frequency of a PSC beam. Compared to concrete beams without prestressing force, PSC beams exhibited an appreciable increase in the natural frequency. In addition, Nabil and Ross (1996) conducted laboratory experiments to assess the dynamic characteristics of beam specimens with a hollow section. With the application of prestressing force to the beam specimens using a tendon placed in the parabolic profile, the natural frequency increased by a maximum of around 22%. Furthermore, Saiidi *et al.* (1994) performed laboratory experiments on a few girders in the Golden Valley Bridge and reported a decrease in the natural frequency owing to the loss of prestressing force.

On the other hand, some studies (Hamed and Frostig 2006, Morassi and Tonon 2008, Whelan *et al.* 2010) concluded that the prestressing force had little influence on the natural frequency of PSC beams. The classical models are somewhat deficient in predicting variations in the natural frequency of a PSC beam due to the prestressing force. Thus, Hamed and Frostig (2006) proposed a nonlinear dynamic analysis model that considers the effect of the compressive force and eccentricity of a tendon cable in a PSC beam and showed that the magnitude of the prestressing force does not influence the natural frequency

\*Corresponding author, Assistant Professor

E-mail: [jh.lee@inha.ac.kr](mailto:jh.lee@inha.ac.kr)

<sup>a</sup> Ph.D., Professor

E-mail: [sbshin@inha.ac.kr](mailto:sbshin@inha.ac.kr)

<sup>b</sup> Ph.D., Director

E-mail: [jangjae@nate.com](mailto:jangjae@nate.com)

of the PSC beam. Morassi and Tonon (2008) and Whelan *et al.* (2010) adopted the result of Hamed and Frostig (2006) and neglected the prestressing effect in the natural frequency in PSC beams.

These two opposing viewpoints on the same physical problem indicate that the general understanding of the effect of the prestressing force on the natural frequency of structures, particularly in actual PSC bridges, remains inadequate. To narrow the gap between the two opposing viewpoints, Dall'asta (1996, 2000) presented an analytical model to compute the natural frequency of a thin-walled beam with a prestressing tendon. This analytical model was based on the equation of motion with a frictionless bond between the steel tendon and the three-dimensional continuum. Dall'asta and Leoni (1999) concluded that the application of a prestressing force to a beam decreased its natural frequency, but the magnitude of this decrease was negligible. However, Dall'asta and Leoni (1999) did not account for the  $P-\Delta$  effects caused by an initial deformation on the variation in the stiffness of PSC beams. Law and Lu (2005) attempted to identify the prestressing effect based on the time-domain responses of a PSC beam. They applied a prestressing force only to the center of the section, which is seldom the case in actual bridges. Jaiswal (2008) investigated the effect of prestressing on the flexural natural frequency of a beam using the finite element technique. Jaiswal (2008) concluded that for a beam with a bonded tendon, the prestressing force does not have any appreciable effect on the first natural frequency, while for a beam with an unbonded tendon, the first natural frequency changes with the prestressing force and eccentricity of the tendon.

The previous analytical studies are indistinct and dependent on mathematical assumptions. Thus, an adequate analytical method should be developed for application to real PSC bridges. To this end, a finite element formulation of the dynamic equation of motion is proposed considering the additional geometric stiffness imparted by prestressing. This finite element formulation is examined using the laboratory test data available in the literature. Then, the formulation is applied to actual PSC bridges to examine the effect of prestressing on the natural frequencies of the bridges. The results of the study show that the change in the natural frequencies of actual PSC bridges under an applied prestressing force is negligible, which is inconsistent with the results obtained in laboratory-scale PSC specimens.

## 2. Dynamic equation of motion considering prestressing effects

### 2.1 Equation of motion of a prestressed beam

This study assumed that the tendon force is constant along the length of the beam with homogeneous and isotropic materials of the prestressing tendon in a beam. The stresses generated in the beam can be divided into normal and geometric stresses induced by the deformation of the beam and tension of the tendon, respectively. The principle of virtual work is applied to the beam-tendon system, and the following equation is derived according to Dall'asta and Leoni (1999):

$$\begin{aligned} & \int_V \mathbf{S} \cdot \hat{\mathbf{E}} \, dV + \tau(a) \hat{a} L_0 + \int_V \mathbf{T}_0 \cdot \mathbf{U}^T \hat{\mathbf{U}} \, dV \\ & + \frac{\tau_0}{L_0} \int_0^L (\mathbf{I} - \mathbf{g}_c \otimes \mathbf{g}_c) \cdot (\mathbf{U}^h \mathbf{h}' \otimes \hat{\mathbf{U}}^h \mathbf{h}') \, dV \quad (1) \\ & = \int_V \rho_0 (\mathbf{b} - \ddot{\mathbf{u}}) \cdot \hat{\mathbf{u}} \, dV + \int_S \mathbf{t} \cdot \hat{\mathbf{u}} \, dS \end{aligned}$$

where  $\mathbf{S}$  denotes the stress tensor of the beam;  $\tau(a)$  the uniform tendon stress due to beam deformation;  $a$  the axial strain of the tendon;  $\tau_0$  and  $L_0$  the initial stress and length of the tendon, respectively;  $\mathbf{T}_0$  the Cauchy stress tensor;  $\mathbf{U}$  and  $\mathbf{U}^h$  the deformation gradients of the beam and tendon path, respectively;  $\mathbf{h}$  the position vector of the tendon in its reference configuration;  $\mathbf{g}_c$  the tangent unit vector of the initial tendon path;  $\rho_0$  the unit mass of the beam;  $\mathbf{b}$  and  $\mathbf{t}$  the body and traction forces applied to the beam, respectively;  $\hat{\mathbf{E}}$  and  $\hat{\mathbf{u}}$  the virtual strain and displacement tensors of the beam, respectively; and  $\hat{\mathbf{a}}$  the virtual strain of the tendon.

The equation of motion, Eq. (1), accounts for the tendon profile along the beam and can reflect the actual situation of the beam-tendon system. That is, the fourth term in Eq. (1) represents the geometric stiffness attributable to the tendon force, which increases the stiffness of the beam-tendon system. However, Eq. (1) does not consider the initial beam deformation caused by prestressing of the tendon. Thus, the third term of Eq. (1), which contains the Cauchy stress tensor, reduces the stiffness of the beam-tendon system, leading to a decrease in the natural frequencies of the system.

### 2.2 Linear geometric stiffness with initial beam deformation

Prestressing tendons in actual PSC beams are typically arranged in a linear manner with a constant eccentricity or a parabolic profile toward the downward direction. Thus, an initial upward vertical displacement occurs in a direction opposite to that of the applied load. This initial deformation leads to the development of the  $P-\Delta$  moment with a sign different from that of the flexural moment caused by the applied loads and, thus, increases the flexural stiffness of the beam. In this study, the direction or sign of the Cauchy stress  $\mathbf{T}_0$  in Eq. (1) is employed to account for the increase in the beam stiffness due to prestressing of the tendon.

Fig. 1 shows a beam with an upward distributed load induced by the prestressing force applied to the tendon. The distributed load induced by the prestressing of the tendon  $q_{pre}$  generates a vertical displacement  $w_{pre}$ , which leads to the development of the moment  $T \cdot w_{pre}$  due to the axial force  $T$ . The moment  $T \cdot w_{pre}$  acts in a direction opposite to that of the moment induced by the applied load  $q$ . When the deflection induced by the applied load  $w$  is smaller than  $w_{pre}$ ,  $\mathbf{T}_0$  becomes positive, leading to an increase in the stiffness of the beam.

### 2.3 Undamped dynamic equation of motion

Based on Eq. (1), a finite element formulation of the undamped dynamic equation of motion is derived in the

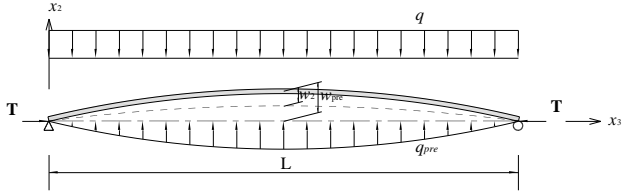


Fig. 1 Beam with an initial displacement induced by prestressing of tendon

Fortran programming environment. Fig. 2 shows the coordinate system used for deriving the undamped dynamic equation of motion of the beam-tendon system. The first term of Eq. (1) is expressed using the Euler-Bernoulli beam theory and neglecting shear deformation of the beam. On the other hand, the Timoshenko beam theory, which accounts for the effects of both the shear force and bending moment, is suitable for describing the behavior of deep beams defined as the ratio of clear span to depth less than 4 (ACI 318-14), but the contribution of the shear to the overall deflection is insignificant in slender beams involved in the study. With the curvature  $\theta'$  in the Euler-Bernoulli beam model, the first term of Eq. (1) can be expressed as follows:

$$\int_0^L \mathbf{D}\theta' \cdot \hat{\theta}' dx_3 = \mathbf{d}^T \left( \int_0^L \mathbf{B}^T \mathbf{D}\mathbf{B} dx_3 \right) \hat{\mathbf{d}} \quad (2)$$

where  $\theta' = (\theta'_1 \theta'_3)^T$ ,  $\mathbf{d} = (w_{2i} \theta_{1i} \theta_{3i} w_{2j} \theta_{1j} \theta_{3j})$ ,  $\mathbf{D} = \text{diag}[EI_{22}, GJ]$ , and  $\mathbf{B}$  represents the relationship between strain and displacement with shape functions, as follows:

$$\mathbf{B} = \begin{bmatrix} \frac{d^2}{dx_3^2} N_1(x_3) & \frac{d^2}{dx_3^2} N_2(x_3) & 0 & \frac{d^2}{dx_3^2} N_3(x_3) & \frac{d^2}{dx_3^2} N_4(x_3) & 0 \\ 0 & 0 & \frac{d}{dx_3} N_5(x_3) & 0 & 0 & \frac{d}{dx_3} N_6(x_3) \end{bmatrix} \quad (3)$$

where the shape functions of  $N_1$  to  $N_4$  are derived using Hermitian polynomials and those of  $N_5$  and  $N_6$  using Lagrangian polynomials. The second term of Eq. (1), which represents the stiffness of the prestressing tendon, is expressed in the same manner as the first term by using a transformed section.

Limiting the beam displacement  $w$  along the vertical direction, the third term of Eq. (1), that is, the linear geometric stiffness due to an axial force, can be expressed as follows:

$$\int_0^L T w'_2 \hat{w}'_2 dx_3 = \kappa \mathbf{d}^T \left( \int_0^L T \mathbf{N}_G^T \mathbf{N}_G dx_3 \right) \hat{\mathbf{d}} \quad (4)$$

The coefficient  $\kappa$  that indicates the sign of geometric stiffness under an applied axial force  $T$  is defined as follows:

$$\kappa = \begin{cases} -1 & w_2 \geq w_{pre} \\ +1 & w_2 < w_{pre} \end{cases} \quad (5)$$

where  $w_{pre}$  denotes the upward deflection of the beam due to the prestressing of the tendon.  $\mathbf{N}_G$  in Eq. (4) is the

derivative of the shape functions:

$$\mathbf{N}_G = \begin{bmatrix} \frac{d}{dx_3} N_1(x_3) & \frac{d}{dx_3} N_2(x_3) & 0 & \frac{d}{dx_3} N_3(x_3) & \frac{d}{dx_3} N_4(x_3) & 0 \end{bmatrix} \quad (6)$$

The fourth term of Eq. (1), which represents the geometric stiffness of the prestressed tendon, can be simplified using the beam strain  $w'_2$ :

$$\int_0^L \frac{T}{\ell^3} w'_2 \hat{w}'_2 dx_3 = \mathbf{d}^T \left( \int_0^L \frac{T}{\ell^3} \mathbf{N}_{Gc}^T \mathbf{N}_{Gc} dx_3 \right) \hat{\mathbf{d}} \quad (7)$$

where  $\ell = \sqrt{(x'_{c2})^2 + 1}$ , and  $\mathbf{N}_{Gc}$  is expressed using the derivative of the shape functions

$$\mathbf{N}_{Gc} = \begin{bmatrix} \frac{d}{dx_3} N_1(x_3) & 0 & 0 & \frac{d}{dx_3} N_3(x_3) & 0 & 0 \end{bmatrix} \quad (8)$$

Neglecting the body force, the force terms in Eq. (1) can be expressed by:

$$-\int_V \rho_0 \ddot{\mathbf{u}} \cdot \hat{\mathbf{u}} dV + \int_S \mathbf{t} \cdot \hat{\mathbf{u}} dS = \int_0^L \mathbf{N}^T \mathbf{q} \cdot \hat{\mathbf{d}} dx_3 - \int_0^L \mathbf{N}^T \mathbf{L} \mathbf{N} \ddot{\mathbf{d}} \cdot \hat{\mathbf{d}} dx_3 = \left( \mathbf{f} - \int_0^L \mathbf{N}^T \mathbf{L} \mathbf{N} \ddot{\mathbf{d}} dx_3 \right) \cdot \hat{\mathbf{d}} \quad (9)$$

where  $\mathbf{q}$  is the distributed load vector, and  $\mathbf{L}$  is the mass matrix per unit length.

Therefore, the final undamped equation of motion is derived as follows:

$$\mathbf{M} \ddot{\mathbf{d}}(t) + (\mathbf{K}_B + \delta \mathbf{K}_G + \mathbf{K}_{Gc}) \mathbf{d}(t) = \mathbf{f} \quad (10)$$

where  $\mathbf{K}_B$  is the normal stiffness of the beam,  $\delta \mathbf{K}_G$  is the geometric stiffness due to the axial force, and  $\mathbf{K}_{Gc}$  is the geometric stiffness of the tendon due to the prestressing of the tendon. The normal and geometric stiffnesses of the beam-tendon system are expressed as follows:

$$\mathbf{K}_B = \int_0^L \mathbf{B}^T \mathbf{D}\mathbf{B} dx_3 \quad (11a)$$

$$\delta \mathbf{K}_G = \kappa \int_0^L T \mathbf{N}_G^T \mathbf{N}_G dx_3 \quad (11b)$$

$$\mathbf{K}_{Gc} = \int_0^L \frac{T}{\ell^3} \mathbf{N}_{Gc}^T \mathbf{N}_{Gc} dx_3 \quad (11c)$$

The  $\mathbf{M}$  and  $\mathbf{f}$  matrixes, which present the mass and external force in the beam system, respectively, are as follows:

$$\mathbf{M} = \int_0^L \mathbf{N}^T \mathbf{L} \mathbf{N} dx_3 \quad (12a)$$

$$\mathbf{f} = \int_0^L \mathbf{N}^T \mathbf{q} dx_3 \quad (12b)$$

Thereafter, the eigenvalue equation, which determines the natural frequencies and mode shapes of the beam-

tendon system, can be determined using the following equation:

$$(\mathbf{K}_B + \delta\mathbf{K}_G + \mathbf{K}_{Gc})\boldsymbol{\phi}_j = \omega_j^2\mathbf{M}\boldsymbol{\phi}_j \quad (13)$$

### 3. Validation of proposed model with laboratory test data

Mode data obtained using the proposed model, Eq. (13), were compared with the laboratory experiment data obtained by Nabil and Ross (1996). In the experiment, Nabil and Ross (1996) included rectangular, I-shaped, and T-shaped cross sections. Fig. 3 shows the shapes and dimensions of the cross sections of the three beam specimens. All the specimens were defined as 5 m in length under a simply-supported condition. The prestressing force was applied using two of seven wire strands 8 mm in diameter, which were placed in a parabolic profile along the length of the beam. The natural frequencies of the first mode of each type of cross section were compared with those obtained using the proposed method with variations in the prestressing force.

Fig. 4 shows the variation of the first natural frequencies of the specimens obtained in the experiment and the proposed method with increasing prestressing force. The experimental and analytical data of the beams with rectangular and I-shaped sections exhibited excellent agreement throughout the range of applied prestressing forces, as shown in Figs. 4(a)-(b), respectively. The first natural frequencies of the rectangular and I-shaped sections increase almost linearly with increasing prestressing force. The T-shaped section also exhibits a linear increasing trend with the prestressing force, but there exists a constant gap between the experimental data and the data obtained with the proposed method, as shown in Fig. 4(c). For the T-shaped beam without prestressing force, the natural frequency of the first mode obtained using a commercial finite element software matched that obtained using the proposed method. Thus, the discrepancy between the experimental and analytical data in case of the T-shaped section might be attributed to some differences between the given design information and real conditions, such as the self-weight and boundary conditions of the specimen. Consequently, the data obtained with the proposed method exhibit reasonable agreement with the experimental data, with a linear increasing trend in the first natural frequency along with increasing prestressing force.

### 4. Applications to practical PSC beam bridges

#### 4.1 Sample PSC railway bridges

To examine the effect of the prestressing force in actual bridges, analytical studies using the proposed method were conducted on typical PSC beam railway bridges designed for use in the field. Fig. 5 shows the two types of PSC bridges defined as A-type and B-type according to the bridge widths of 10.9 m and 10.6 m, respectively. The A-

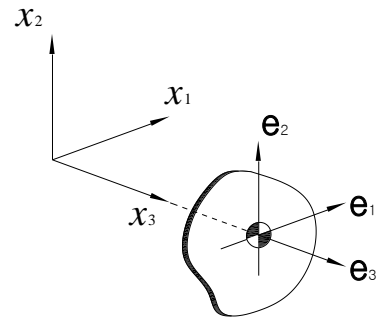


Fig. 2 Coordinate system with respect to cross section of a beam

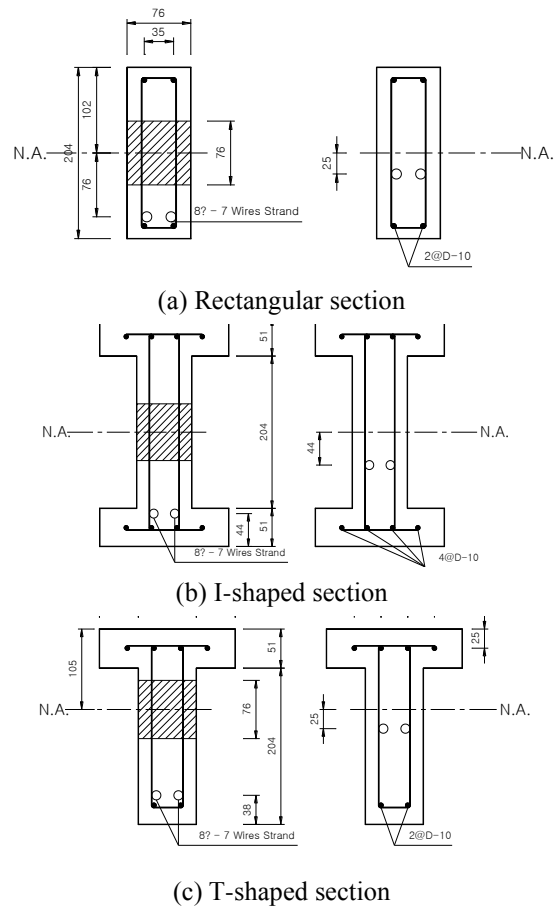


Fig. 3 Sections and dimensions of tested three beams (units: mm)

type bridge consisted of six PSC girders and the B-type bridge of five PSC girders. The simply-supported span lengths of the A-type bridge were set to 20 m, 23 m, and 25 m, denoted as A-20, A-23, and A-25, respectively. The span length of the B-type bridge under the simply-supported condition was set to 25 m, denoted as B-25. Fig. 6 shows the shapes and dimensions of the four sections, A-20, A-23, A-25, and B-25, employed in the study. The sections of the girders are similar to those of the AASHTO-PCI *Bulb-Tee* girders (PCI bridge design manual 2003) but have different sectional dimensions. The prestressing tendons were placed in a parabolic arrangement, as presented in Fig. 7. The material and sectional properties of each girder type, including compressive strength ( $f_c$ ), moment of inertia ( $I$ ),

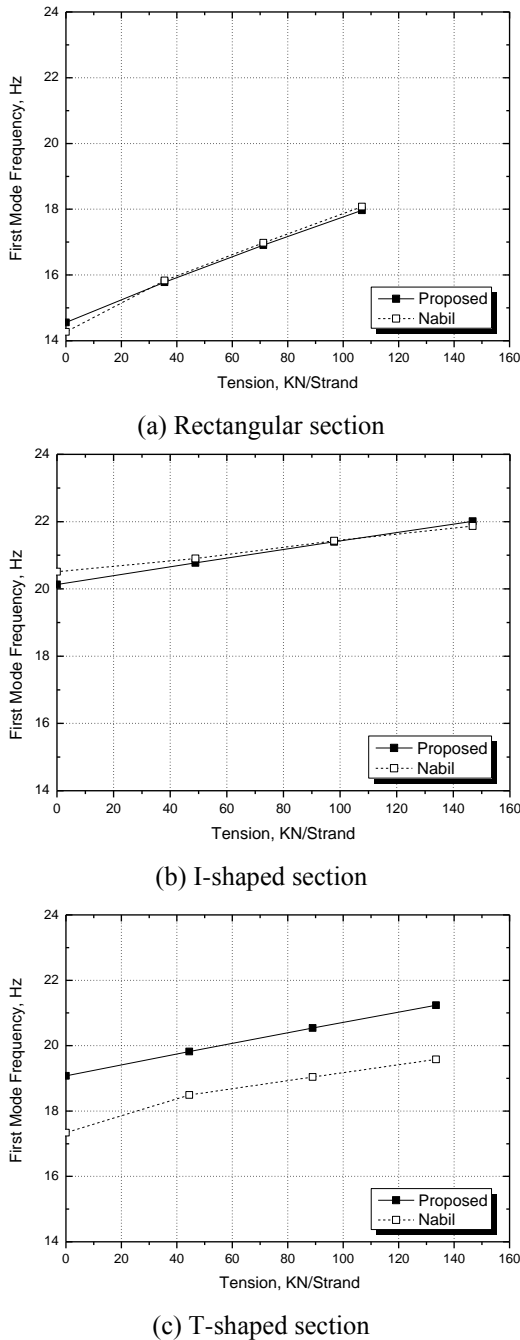


Fig. 4 Comparisons of variations in the first natural frequencies of experiments with those of proposed method

Table 1 Material and sectional properties of bridges

	A-20	A-23	A-25	B-25
$f'_c$ (MPa)	Girder	35		40
	Slab		27	
Density (kg/m <sup>3</sup> )		2,500		
$I$ (m <sup>4</sup> )	0.7476		1.0295	1.1237
$J$ (m <sup>4</sup> )	0.0433		0.0426	0.0467

and torsional constant ( $J$ ), are summarized in Table 1. In addition to the mass of the girder and slab, the loads of the rail (120 kg/m), ballast (800 kg/m), and sleeper (762 kg/m) are included.

Table 2 Natural frequencies obtained with the proposed finite element model

	A-20	A-23	A-25	B-25
$f_0$ (Hz)	9.017	6.403	6.171	6.541
$f_p$ (Hz)	9.118	6.515	6.262	6.640
$f_p/f_0$	1.011	1.018	1.015	1.015

#### 4.2 Natural frequency of PSC bridges

The four types of railway PSC bridges were modeled as grillage finite elements using the proposed finite element method. Table 2 lists the first natural frequencies obtained using the proposed method, where  $f_0$  and  $f_p$  represent the first natural frequencies without and with the prestressing force, respectively. The ratio of  $f_p$  to  $f_0$ , which ranges from 1.011 to 1.018, shows little difference among the types of girders. This indicates that the influence of the prestressing force on the variation of the natural frequency is negligible. The influence of the prestressing force on the natural frequency in the actual PSC bridges was different from that in the laboratory test data discussed in the previous Section 3, which showed a linear increasing trend of the first natural frequency with increasing prestressing force.

#### 4.3 Discussion on the two contrasting results

The results of the present study indicate that as the prestressing force increased, the natural frequency of the beam increased in the laboratory test data but hardly changed in case of the actual PSC bridges. Thus, this study assessed the influence of the stiffness and mass components of the beam, which mainly determine the natural frequency of the beam. Table 3 shows the ratio of the prestressing force to the total weight of the beam in the cases of the laboratory tests (Nabil and Ross, 1996) and the actual PSC beam bridges. Surprisingly, the ratio of the prestressing force to the total weight ranged from approximately 34.9 to 54.4 in the laboratory tests and from 1.08 to 1.42 in the actual PSC girders. In other words, the magnitude of the prestressing force applied to the beam with respect to the total self-weight of the beam differed considerably between the laboratory tests and the actual PSC bridges.

Therefore, a parametric study was conducted to evaluate the variation in the natural frequency with the increase in the ratio of the prestressing force to the total weight ( $T/W$ ) for the rectangular section used by Nabil and Ross (1996) and the aforementioned four types of actual PSC bridges. Fig. 8 shows the variations in the natural frequency of the beam and vertical deflection at mid-span with increasing  $T/W$ . The left- and right-hand-side vertical coordinates indicate the ratio of the first natural frequency and the deflection of the beam with the prestressing force  $T$  to those without  $T$ , respectively. The natural frequency of the beam specimen employed by Nabil and Ross (1996) increases almost linearly with increasing  $T/W$  from zero to 100, as denoted by the solid line in Fig. 8(a). The dotted line in Fig. 8(a), which corresponds to the right-hand-side vertical coordinate, denotes the decrease in the vertical deflection

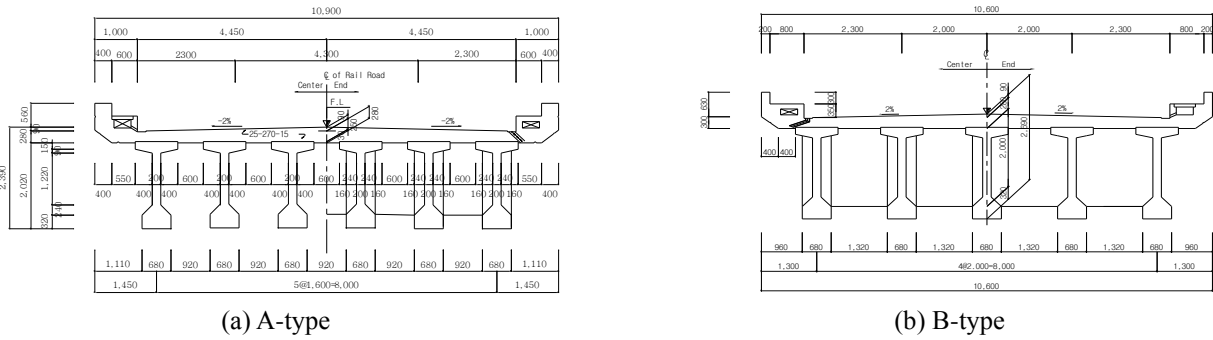


Fig. 5 Cross sections of bridges (units: mm)



Fig. 6 Details of girder sections (units: mm)

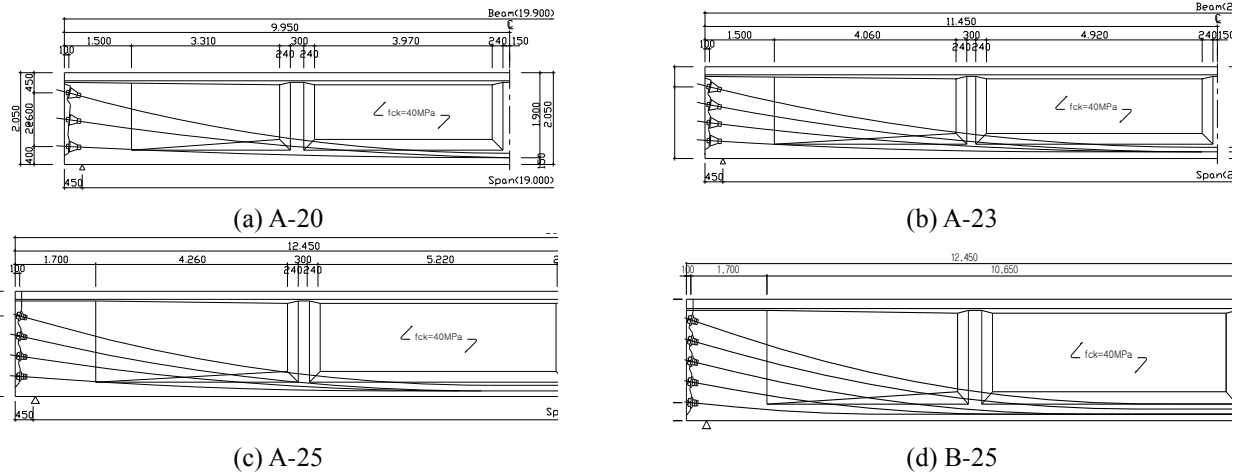
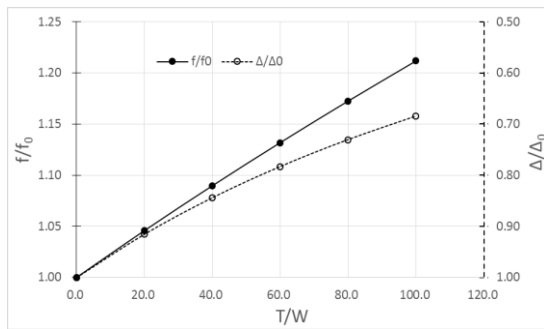


Fig. 7 Details of tendon layouts (units: mm)

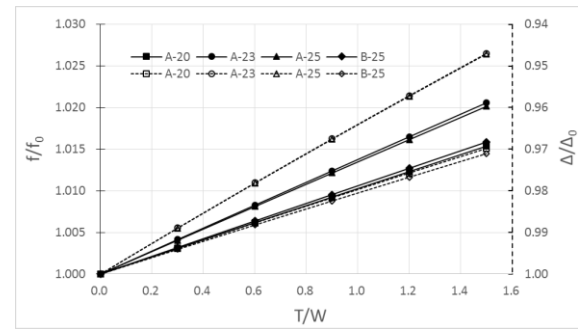
with increasing  $T/W$ . This decrease in the deflection is attributed to an increase in the stiffness under application of the prestressing force, but it is not linear unlike the variation of the natural frequency. When  $T/W$  is 100 in the laboratory test, the natural frequency increases by approximately 22%, and the deflection decreases by 32%. For the actual PSC girder, Fig. 8(b) shows the increase in the natural frequency and the decrease in the deflection with increasing  $T/W$ . The magnitude of change in the natural frequency and the deflection, which are smaller than approximately 2.0% and 5.0%, respectively, are negligible. As a result, the natural

Table 3 Ratio of prestressing force to total beam weight

	Nabil and Ross (1996)		PSC bridges				
	Rectangular	I-type	T-type	A-20	A-23	A-25	B-25
Total weight ( $W$ , kN)	1.91	4.21	3.07	4,450	5,118	5,788	5,251
Total prestressing force ( $T$ , kN)	103.80	146.85	133.50	4,817	6,515	6,380	7,475
Prestressing force / Weight ( $T/W$ )	54.35	34.88	43.49	1.08	1.27	1.10	1.42



(a) Nabil and Ross (1996): Rectangular section



(b) PSC beam bridges

Fig. 8 Variation in natural frequency and vertical deflection with an increase in the ratio of the prestressing force to total weight of the beam

frequency changes as the prestressing force increases, but the ratio of the change strongly depends on the magnitude of the prestressing force relative to the total weight of the structure. That is, the laboratory specimens with relatively small weight of the beam exhibit a considerable change in the natural frequency as the prestressing force changes. However, the change in the natural frequencies of the actual PSC bridges with high total weight relative to the prestressing force is negligible.

## 5. Conclusions

The paper investigated the effects of prestressing force on the natural frequency of PSC bridges. A finite element formulation was introduced based on the principle of virtual work to define the modal equation of a beam-tendon system. The proposed equation introduced two terms of geometric stiffness, which can account for the effects of axial force and deformation of the prestressing tendon on the stiffness of the beam-tendon system.

The developed finite element formulation was examined with experimental data obtained in laboratory-scale specimens. The first natural frequencies of the beam specimens with rectangular and I-shaped sections obtained in the experiment agreed well with the corresponding values obtained using the proposed method throughout the range of applied prestressing force. The natural frequencies increased linearly with increasing prestressing force. The T-shaped section, even though there is a constant gap between the given information and the analytical data obtained from the proposed method, showed a linear increasing trend with the prestressing force.

Furthermore, this study examined the effect of the prestressing force in four typical designs of PSC beam railway bridges with the widths of 10.6 m and 10.9 m and the span lengths of 20 m, 23 m, and 25 m. The ratio of the first natural frequencies with the prestressing force to those without the prestressing force ranged from 1.011 to 1.018. This indicates that different from the laboratory specimens, the effect of the prestressing force on the first natural frequency is negligible in the actual PSC bridges. In addition, the first natural frequencies of the PSC bridges showed little difference among the types of girders.

Therefore, a parametric study was conducted to evaluate the variation in the natural frequency as well as vertical deflection in terms of the ratio of the prestressing force to the total weight of a structure. The laboratory-scale beam specimens with low self-weights relative to the prestressing force showed considerable changes in the natural frequency and vertical deflection of the beam. The natural frequency of the beam specimens increased almost linearly with the increase in the ratio of the prestressing force to the total weight of the beam, while the vertical deflection decreased due to the increase in the stiffness under application of the prestressing force. However, the natural frequency and vertical deflection of the actual PSC bridges, which had high self-weights with respect to the applied prestressing force, hardly changed. The changes in the natural frequency and the deflection were smaller than approximately 2.0% and 5.0%, respectively. In conclusion, the effect of the prestressing force depends strongly on the magnitude of the prestressing force relative to the total weight of a structure. Thus, changes in the natural frequency and vertical deflection are not good indicators for evaluating the safety condition and serviceability of PSC beam bridges.

## Acknowledgment

This research was supported by a grant(19SCIP-B128492-03) from Smart Civil Infrastructure Research Program funded by Ministry of Land, Infrastructure and Transport of Korean government.

## References

- Abbasnia, R., Mirzaee, A., and Shayanfar, M. (2015), "Simultaneous identification of moving loads and structural damage by adjoint variable", *Struct. Eng. Mech.*, **56**(5), 871-897. <https://doi.org/10.12989/sem.2015.56.5.871>.
- ACI 318-14. (2014), "Building code requirements for structural concrete", American Concrete Institute, Framington Hills, USA.
- Dall'asta, A. (1996), "On the coupling between three dimensional bodies and slipping cables", *Int. J. Solids Struct.*, **33**(24), 3587-3600. [https://doi.org/10.1016/0020-7683\(95\)00204-9](https://doi.org/10.1016/0020-7683(95)00204-9).
- Dall'asta, A. (2000), "Dynamics of elastic bodies prestressed by internal slipping cables", *Int. J. Solids Struct.*, **37**, 3421-3438. [https://doi.org/10.1016/S0020-7683\(99\)00032-3](https://doi.org/10.1016/S0020-7683(99)00032-3).

- Dall'asta, A and Leoni, G. (1999), "Vibration of beams prestressed by internal frictionless cables", *J. Sound Vib.*, **222**(1), 1-18. <https://doi.org/10.1006/jsvi.1998.2066>.
- Falati, S. and Williams, M.S. (1998), "Vibration tests on a model post-tensioned concrete floor: Interim report", Report No. OUEL 2155/98, Department of Engineering Science, University of Oxford, United Kingdom.
- Gao, Q., Yang, M.G., and Qiao, J.D. (2017), "A multi-parameter optimization technique for prestressed concrete cable-stayed bridges considering prestress in girder", *Struct. Eng. Mech.*, **64**(5), 567-577. <https://doi.org/10.12989/sem.2017.64.5.567>.
- Goremikins, V., Rocens, K., Serdjuks, D., and Gaile, L. (2013), "Experimental determination of natural frequencies of prestressed suspension bridge model", *Constr. Sci.*, **14**(1), 2-37. <https://doi.org/10.2478/cons-2013-0005>.
- Hamed, E. and Frostig, Y. (2006), "Natural frequencies of bonded and unbonded prestressed beams-prestress force effects", *J. Sound Vib.*, **295**(1-2), 28-39. <https://doi.org/10.1016/j.jsv.2005.11.032>.
- Hop, T. (1991), "The effect of degree of prestressing and age of concrete beams on frequency and damping of their free vibration", *Mater. Struct.*, **24**(3), 210-220. <https://doi.org/10.1007/BF02472987>.
- Jaiswal, O.R. (2008), "Effect of prestressing on the first natural frequency of beams", *Struct. Eng. Mech.*, **28**(5), 515-524. <https://doi.org/10.12989/sem.2008.28.5.515>.
- James, M.L., Lutes, L.D., and Smith, G.M. (1964), "Dynamic properties of reinforced and prestressed concrete structural components", *ACI J. Proc.*, **61**(11), 1359-1380.
- Law, S.S. and Lu, Z.R. (2005), "Time domain responses of a prestressed beam and prestress identification", *J. Sound Vib.*, **288**(4-5), 1011-1025. <https://doi.org/10.1016/j.jsv.2005.01.045>.
- Lee, J.H., Park, Y.M., Jung, C.Y., Kim, J.B. (2017), "Experimental and measurement methods for the small-scale model testing of lateral and torsional stability", *Int. J. Conc. Struct. Mater.* **11**(2), 377-389. <https://doi.org/10.1007/s40069-017-0198-3>.
- Morassi, A. and Tonon, S. (2008), "Dynamic testing for structural identification of a bridge", *ASCE J. Bridge Eng.*, **13**(6), 573-585. [https://doi.org/10.1061/\(ASCE\)1084-0702\(2008\)13:6\(573\)](https://doi.org/10.1061/(ASCE)1084-0702(2008)13:6(573)).
- Nabil, F.G. and Ross, B. (1996), "Dynamic characteristics of post-tensioned girders with web openings", *ASCE J. Struct. Eng.*, **122**(6), 643-650. [https://doi.org/10.1061/\(ASCE\)0733-9445\(1996\)122:6\(643\)](https://doi.org/10.1061/(ASCE)0733-9445(1996)122:6(643)).
- Noble, D., Nogal, M., O'Connor, A.J., and Pakrashi, V. (2015), "The effect of post-tensioning force magnitude and eccentricity on the natural bending frequency of cracked post-tensioned concrete beams", *J. Phys.: Conf. Ser.* **628**(2015), 1-8. <https://doi.org/10.1088/1742-6596/628/1/012047>.
- Noh, M.H., Seong, T.R., Lee, J., and Park, K.S. (2015), "Experimental investigation of dynamic behavior of prestressed girders with internal tendons", *Int. J. Steel Struct.*, **15**(2), 401-414. <https://doi.org/10.1007/s13296-015-6011-8>.
- PCI bridge design manual. (2003). Precast/Prestressed Concrete Institute, Chicago, Illinois, USA
- Rogers, L.P., Seo, J. (2016). "Vulnerability sensitivity of curved precast-concrete I-girder bridges with various configurations subjected to multiple ground motions", *J. Bridge Eng.*, **22**(2). [https://doi.org/10.1061/\(ASCE\)BE.1943-5592.0000973](https://doi.org/10.1061/(ASCE)BE.1943-5592.0000973).
- Saiidi, M., Douglas, B., and Feng, S. (1994), "Prestress force effect on vibration frequency of concrete bridges", *ASCE J. Struct. Eng.*, **120**(7), 2233-2241. [https://doi.org/10.1061/\(ASCE\)0733-9445\(1996\)122:4\(460.x\)](https://doi.org/10.1061/(ASCE)0733-9445(1996)122:4(460.x)).
- Seo, J., Linzell, D.G. (2011). "Nonlinear seismic response and parametric examination of horizontally curved steel bridges using 3D computational models", *J. Bridge Eng.*, **34**(3), 220-231. [https://doi.org/10.1061/\(ASCE\)BE.1943-5592.0000345](https://doi.org/10.1061/(ASCE)BE.1943-5592.0000345).
- Seo, J., Linzell, D.G. (2012). "Horizontally curved steel bridge seismic vulnerability assessment", *Eng. Struct.*, **34**, 21-32. <https://doi.org/10.1016/j.engstruct.2011.09.008>.
- Shin, S., Koo, M.S., Lee, H.K., and Kwon, S.J. (2010), "Variation of eigen-properties of a PSC bridge due to prestressing force", *Bridge Maintenance, Safety, Management and Life-Cycle Optimization: Proceedings of the 5th International IABMAS Conference*, Philadelphia, USA, July.
- Turkeli, E. and O zturk, H. T. (2017), "Optimum design of partially prestressed concrete beams using genetic algorithms", *Struct. Eng. Mech.*, **64**(5), 579-589. <https://doi.org/10.12989/sem.2017.64.5.579>.
- Whelan, M.J., Gangone, M.V., Janoyan, K.D., Hoult, N.A., Middleton, C.R., and Soga, K. (2010), "Wireless operational modal analysis of a multi-span prestressed concrete bridge for structural identification", *Smart Struct. Syst.*, **6**(5-6), 579-593. [https://doi.org/10.12989/sss.2010.6.5\\_6.579](https://doi.org/10.12989/sss.2010.6.5_6.579).

CC